European Journal of Pharmaceutics and Biopharmaceutics 77 (2011) 392–397

Contents lists available at ScienceDirect

European Journal of Pharmaceutics and Biopharmaceutics

journal homepage: www.elsevier.com/locate/ejpb

Research paper

Nanoparticles attenuate P-glycoprotein/MDR1 function in A549 human alveolar epithelial cells

Johanna J. Salomon, Carsten Ehrhardt *

School of Pharmacy and Pharmaceutical Sciences, Trinity College Dublin, Dublin 2, Ireland

ARTICLE INFO

Article history:
Available online 18 November 2010

Keywords:
A549 cells
Rhodamine 123
Drug transporter
Release study

ABSTRACT

P-glycoprotein/MDR1 (P-gp) is a well-characterised membrane transporter relevant in drug disposition and multi-drug resistance. In this study, we aimed to investigate how far nanoparticulates impair the function of the P-gp transport system and which particle properties govern these interactions.

Expression and function of P-gp was confirmed in A549 cell monolayers. Rhodamine 123 (Rh123) release studies were carried out in the presence of known inhibitors of P-gp function (i.e., cyclosporine A and verapamil), under ATP depletion (NaN_3/DOG) and after acute exposure to nanoparticles (NPs) with different surface modifications, ζ-potentials and sizes (plain, carboxylated, and amine- and sulphate-modified). The cytotoxic potential of NPs on A549 monolayers was evaluated by MTT assay. The effects on P-gp protein level, after incubation with NPs, were investigated by Western blot analysis of A549 cell lysate and supernatant.

Cellular retention of Rh123 was significantly ($P < 0.05$) increased in the presence of carboxylated (100 nm), amine- and sulphate-modified NPs. A slight, but not significant, decrease in Rh123 release was also observed for plain latex and carboxylated (500 nm) NPs. The MTT assay demonstrated that most NPs caused only marginal levels of cytotoxicity (78–88% cell viability); the positively charged amine-NPs, however, were considerably more cytotoxic. Western blot showed that NPs did not cause any cell membrane disruption.

Our findings suggest that nanomaterials can attenuate membrane transporter function depending on their size and surface properties and hence might influence the disposition of xenobiotics as well as endogenous substrates.

1. Introduction

The use of nanotechnologies has expanded rapidly during the last decade and begins to revolutionise the scientific landscape as well as everyday's life. Nanoparticles, nanometre-ranged drug delivery systems, offer opportunities across all areas of medical treatment. Significant advances in cancer diagnostics, imaging and therapy have been developed based on the nanomedicine approach [1,2]. To improve the biodistribution of (particularly anti-cancer) drugs, nanoparticles have been designed for optimal size and surface characteristics to increase their circulation time in the bloodstream. In addition, active targeting strategies using surface-bound ligands directed against selected cellular targets amplify the specificity of these therapeutic nanocarriers [3,4]. It has also been suggested that nanoparticles have the ability to accumulate in cells without being recognised by P-glycoprotein, one of the main mediators of multi-drug resistance, resulting in the increased intracellular concentration of drugs [5]. Nevertheless, at present, we are only beginning to understand the opportunities, challenges and potential hazards of nanomaterials [6].

P-glycoprotein/MDR1 (P-gp) is a 170-kDa membrane glycoprotein encoded by the *ABCB1* gene. It is known to play an important role as an efflux pump in drug disposition, particularly in cancer chemotherapy [7]. P-gp is also expressed in many tissues under physiological conditions, indicating its major role in the cellular transport of a variety of endogenous substrates and therapeutic agents [8,9]. Presently, more than 100 compounds have been identified to be P-gp substrates, of which the majority were basic lipophilic amines [10]. The lung is thought to accumulate lipophilic amines, which strongly suggests that P-gp-mediated efflux plays an important role in pulmonary drug accumulation [11,12]. Interestingly, recent studies on the impact of P-gp on drug disposition after oral inhalation *in vivo* and *in situ* have resulted in quite conflicting data, making this an exciting area for further investigations [13,14].

In this study, we aimed to investigate how far nanoparticulates impair the function of the P-gp transport system and which

* Corresponding author. School of Pharmacy and Pharmaceutical Sciences, Trinity College Dublin, Panoz Institute, Dublin 2, Ireland. Tel.: +353 1 896 2441; fax: +353 1 896 2783.
E-mail address: ehrhardc@tcd.ie (C. Ehrhardt).

0939-6411/$ - see front matter © 2010 Elsevier B.V. All rights reserved.
doi:10.1016/j.ejpb.2010.11.009

particle properties govern these interactions. Commercially available, insoluble latex nanoparticles with various surface and size characteristics were studied in an *in vitro* model of human alveolar epithelial type 2-like cells, A549.

2. Materials and methods

2.1. Materials

A549 cells (ATCC CL-185) were obtained from LGC Promochem (Teddington, UK). All cell culture plastics were obtained from Greiner (Frickenhausen, Germany), with the exception of Lab-Tek chamber slides (Nunc, Roskilde, Denmark). Nanoparticles (L3405, L3280, LB1, L9902 and L0780), mouse monoclonal anti-P-gp antibody (clone F4) and all other chemicals and reagents were purchased from Sigma–Aldrich (Dublin, Ireland).

2.2. Cell culture

A549 (American Type Culture Collection CL-185; LGC Promochem, Teddington Middlesex, UK) cells are derived from a human pulmonary adenocarcinoma [15]. Due to phenotypic similarity to type II alveolar epithelial cells, this cell line has been widely utilised in the studies of alveolar epithelium function [16]. Cells of passage numbers 66–82 were used in this study and were maintained in a 1:1 mixture of Dulbecco's modified Eagle's medium and Ham's nutrient mixture F-12 (DMEM:F-12) supplemented with 5% (v/v) FBS, 100 U/ml penicillin and 100 μg/ml streptomycin. Cells were cultured at 37 °C in 5% CO_2 atmosphere, and culture medium was exchanged every 48 h.

2.3. Rhodamine 123 release studies

Rhodamine 123 (Rh123) release studies were performed using A549 cell monolayers cultured for 5 days in 24-well plates at a density of 40,000 cells/cm^2. Cell layers were washed twice with pre-equilibrated bicarbonated Krebs–Ringer buffer (KRB; composed of 15 mM HEPES, 116.4 mM NaCl, 5.4 mM KCl, 0.78 mM NaH_2PO_4, 25 mM $NaHCO_3$, 1.8 mM $CaCl_2$, 0.81 mM $MgSO_4$ and 5.55 mM glucose; pH 7.4), before being loaded with a 10 μM solution of Rh123 in KRB for 30 min. Next, the Rh123 solution was replaced with freshly prepared, pre-warmed KRB containing the nanoparticles (100 μg/ml) or pharmacological inhibitors (cyclosporine A (CsA) 10 μM; verapamil 10 μM; NaN_3/2-deoxy-D-glucose (DOG) 10 mM). The monolayers were then incubated for 30 min at 37 °C in 5% CO_2 atmosphere, before being washed twice with ice-cold KRB and lysed with a 1% solution of Triton X-100 in KRB.

Fluorescence of samples was analysed in 24-well plates using a fluorescence plate reader (FLUOstar Optima, BMG Labtech, Offenburg, Germany) at excitation and emission wavelengths of 485 and 520 nm, respectively. The samples were diluted with KRB, where appropriate. Rh123 release from untreated A549 cell layers was used as control. For standardisation, the total protein amount of cell layers was determined by bicinchoninic acid (BCA) assay according to the manufacturer's instructions (Pierce, Thermo Scientific, Rockford, USA).

Half-saturation constant (K_m) and maximum release rate (V_{max}) of Rh123 were calculated by fitting the release rate (v) to the following equation by means of non-linear least-squares regression analysis according to the Michaelis–Menten equation (Eadie–Hofstee transformation):

$$v = V_{max} \times (S)/[(K_m + (S)] \quad (1)$$

where (S) was [Rh123].

2.4. Western blot

Cell supernatant (CS) was collected by aspiration from A549 monolayers that have been incubated with KRB containing 100 μg/ml of nanoparticles for 30 min. Cell lysate (CL) was obtained by washing the cell layers three times with ice-cold phosphate saline buffer (PBS), followed by cell homogenisation in 60 μl per well freshly prepared lysis buffer, containing aprotinin (6%) and leupeptin (1%). Samples of CS and CL were sonicated twice for 20 s and centrifuged at 9279 g for 20 min. The total protein amount was determined by Bio-Rad protein assay (Hercules, USA) with bovine serum albumin (BSA) used as standard. Western blot was performed immediately after sample preparation. Samples were standardised to equal protein concentrations, 6 μl of loading buffer was added, and the mixture was heated up to 95 °C for 5 min, before 20 μl of each sample was loaded onto a 6% SDS gel. Electrophoresis was performed for 2 h at 110 V. The protein bands were transferred onto PVDF membranes (Bio-Rad) at 25 V for 30 min. Blots were blocked in PBS containing 5% (w/v) BSA for at least 1 h at room temperature, before overnight incubation with the anti-P-gp primary antibody (1:100) at 4 °C. Membranes were then washed with PBS, and the secondary goat anti-mouse IgG antibody (Promega, Medical Supply, Ireland) in a concentration of 1:13,500 was added for 1 h at room temperature. Peroxidase activity was detected with Immobilon Western Chemiluminescent HRP substrate (Millipore). Signals were documented using a ChemiDoc system (Bio-Rad).

2.5. Analysis of particle size and ζ-potential

Physicochemical properties (i.e., size and ζ-potential) of the nanoparticles were measured before and after the release experiments using a Zetasizer Nano ZS (Malvern, Malvern, UK) at 25 °C and a scattering angle of 173°. Nanoparticles were examined immediately after being suspended in KRB (pH 7.4), before initiation of each Rh123 release experiment. To study changes in physicochemical parameters, 800 μl of the supernatant was analysed for size and ζ-potential measurements at the end of the study. The samples containing nanoparticles were placed in a standard disposable capillary cell (DTS1060, Malvern, UK) for size measurements and ζ-potential, respectively. Average size was calculated from the intensity, volume and number distributions by Dispersion Technology software 5.03 (Malvern). All measurements were taken in triplicate.

2.6. Cell viability assay

The viability of A549 cells was determined by MTT (3-(4,5-dimethyl-thiazol-2-yl)-2,5-diphenyltetrazolium bromide) assay. Cells were seeded at a density of 30,000 cells/cm^2 in 96-well plates and left for 24 h to attach. After 30 min of incubation with nanoparticles (100 μg/ml) suspended in KRB, the cell layers were washed twice with KRB, before 100 μl of fresh KRB and 10 μl of MTT solution (5 mg/ml in KRB) were added to each well. After further incubation at 37 °C for 3 h, the supernatant was removed and cells were dispersed in 50 μl of DMSO. Absorbance was measured at 570 nm by using a microplate reader (FLUOstar Optima).

2.7. Confocal laser scanning microscopy

A549 cell layers were grown on chamber slides at 35,000 cells/cm^2 for 5 days, before cells were being fixed for 10 min with 2% (w/v) paraformaldehyde and incubated for 10 min in 50 mM NH_4Cl, followed by permeabilisation for 8 min with 0.1% (w/v) Triton X-100 in PBS. After 60-min incubation with 200 μl of a 1:500 dilution of monoclonal mouse anti-P-gp antibody, the cell layers

were washed three times with PBS, before incubation with 100 µl of a 1:200 dilution of Alexa Fluor 488-conjugated goat anti-mouse $F(ab')_2$ fragment (Invitrogen) in PBS containing 1% (w/v) BSA. Propidium iodide (1 µg/ml in PBS) was used to counterstain cell nuclei. In the case of F-actin staining, cells were initially incubated for 30 min with nanoparticles (100 µg/ml) suspended in KRB. TRITC-phalloidin was used at a concentration of 500 ng/ml in PBS. After 30 min of incubation, the specimens were again washed three times with PBS and embedded in FluorSave anti-fade medium (Merck, Nottingham, UK). Images were obtained using a confocal laser scanning microscope (CLSM, Zeiss LSM 510, Göttingen, Germany) with the instrument's settings adjusted so that no positive signal was observed in the channel corresponding to the fluorescence of the isotypic controls.

2.8. Statistical analysis

Each experiment was repeated at least in triplicate with cells from three different passages. Results were expressed as mean ± SD of at least three experiments. Two groups were compared using one-way analysis of variance (ANOVA), followed by the Student–Newman–Keuls post hoc test. $P < 0.05$ was considered as significant.

3. Results

3.1. P-gp expression, localisation and activity in A549 cells

Immunocytochemical staining, performed after 5 days of culture of A549 cell layers, showed moderate expression of P-gp in the plasma membrane (Fig. 1A). In addition, a punctuate staining pattern typical for intracellular vesicles or similar substructures was observed (Fig. 1A). Consistent with this observation was a moderate signal of immunoreactive P-gp detected by immunoblot (Fig. 1B).

To investigate P-gp function, A549 cell layers were loaded with Rh123 and the release of the substrate was studied at 37 °C and 4 °C, as well as in the presence of P-gp inhibitors (i.e., CsA and verapamil) and attenuators of energy-dependent translocation events by depletion of ATP (i.e., NaN_3 plus DOG). The difference in fluorescence intensities between the measurements at 37 °C and 4 °C was calculated (depicted in Fig. 2A), and the resulting release was converted by Eadie–Hofstee transformation (a linearisation of the Michaelis–Menten equation) to evaluate the number and activity of transporter sites. The linear plot ($R^2 > 0.97$) shown in Fig. 2B indicates a single transporter site being responsible for the efflux of Rh123. P-gp-mediated efflux was saturable, and kinetic parameters were determined as follows: K_m, 32.91 ± 4.49 µM and V_{max}, 0.057 ± 0.004 nmol/min × mg protein. Cyclosporine A and verapamil almost completely suppressed Rh123 release from A549 cell layers (Fig. 3). A similar effect was observed when A549 monolayers were incubated with NaN_3 plus DOG (Fig. 3).

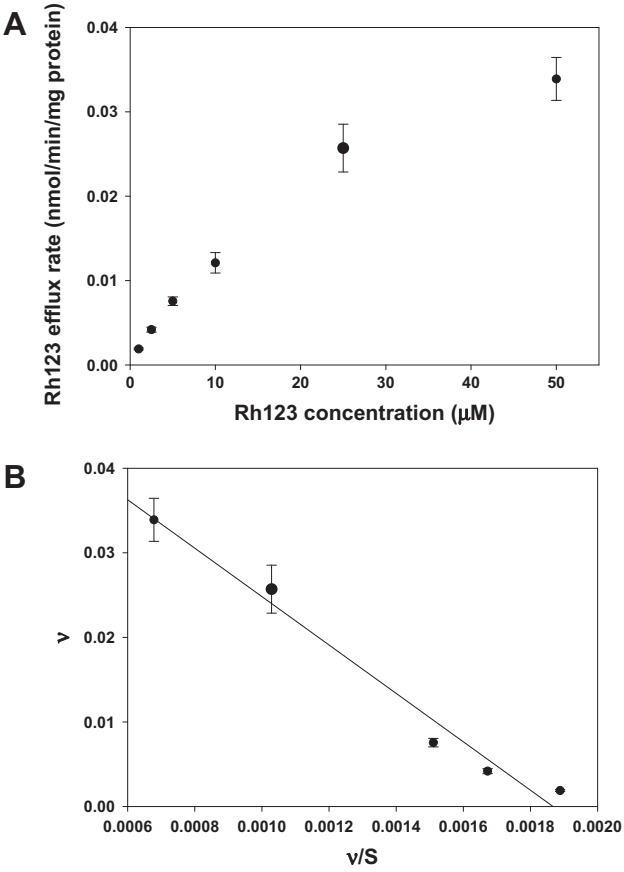

Fig. 2. Kinetic analysis of rhodamine 123 (Rh123) release from A549 cell layers after 5 days of culture. (A) Release of Rh123 was measured for 30 min at 37 °C and 4 °C. The efflux was calculated as the difference in fluorescence signals obtained at the two temperatures and standardised against the total protein amount. (B) Rh123 release data were transformed to an Eadie–Hofstee plot. The linearity of the transformation indicates a single transporter site for Rh123 release from A549 monolayers. Results are expressed as means ± SD ($n = 3$).

3.2. Rh123 efflux in the presence of nanoparticles

Rh123 release studies were then carried out with insoluble nanoparticles of different sizes and surface charges suspended in

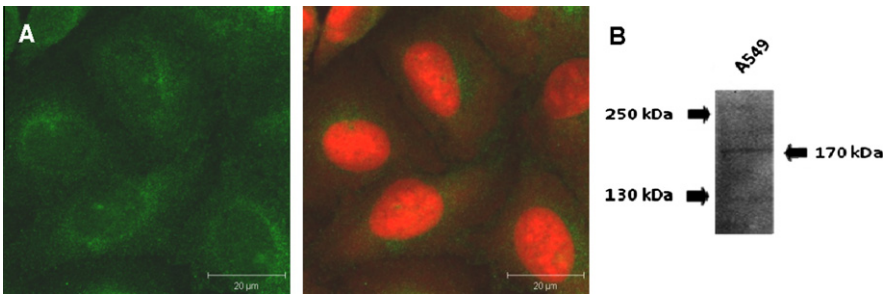

Fig. 1. Expression of P-glycoprotein/MDR1 (P-gp) in plastic-grown A549 human alveolar epithelial cell layers after 5 days of culture. Cells were plated at a density of 3.5×10^4 cells per cm^2 and cultured under liquid-covered culture conditions. (A) Immunolabelling of P-gp. Staining for P-gp (green) is shown using confocal laser scanning microscopy. Nuclei were counterstained with propidium iodide (red). Scale bars represent µm. (B) Immunoblot analysis of P-gp. A single band of 170 kDa can be detected in A549 cell lysate.

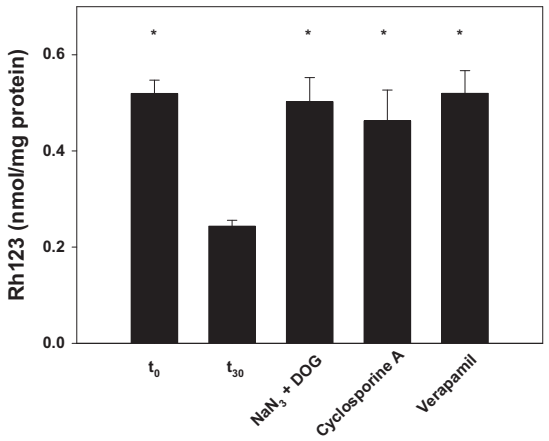

Fig. 3. Effect of cyclosporine A (10 μM), verapamil (10 μM) and NaN_3/2-deoxy-D-glucose (DOG; 10 mM) on rhodamine 123 (Rh123) release from A549 cell layers cultured for 5 days. Cell layers were loaded with Rh123 (10 μM) for 30 min (t_0), and fluorescence was measured after another 30 min of release (t_{30}). Results are expressed as means ± SD from 6 independent experiments. $^*P < 0.01$ versus control buffer alone.

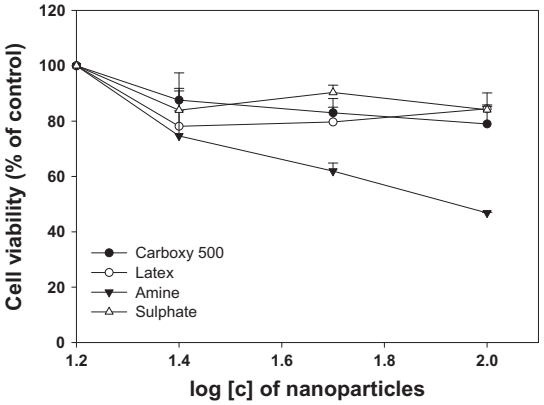

Fig. 5. Cytotoxicity of nanoparticles. A549 cell layers were cultured for 5 days, before being incubated with different nanoparticles (100 μg/ml) for 30 min. Cell viability was assessed by MTT assay and normalised to the level of untreated cells. Results are expressed as means ± SD ($n = 6$).

the incubation buffer at concentrations of 100 μg/ml. Fig. 4 shows the effect of the nanoparticles on Rh123 release from A549 cell layers. Incubation with carboxy (100 nm), amine and sulphate nanoparticles resulted in significantly ($P < 0.01$ and $P < 0.05$, respectively) higher intracellular Rh123 levels after 30 min, indicating an attenuating effect on release by inhibition of the P-gp transport system. Carboxy (500 nm) and unmodified latex particles also decreased Rh123 efflux, albeit those effects were not significant ($P < 0.05$).

3.3. Cytotoxicity assay

In order to investigate whether the observed P-gp attenuating effects resulted from cytotoxic events caused by the nanoparticulates, the viability of A549 cells was tested by MTT assay. Cells were incubated with NPs at concentrations of 25, 50 and 100 μg/ml for 30 min (Fig. 5). Carboxy (500 nm), latex and sulphate particles marginally reduced the cell viability to 79 ± 7%, 78 ± 14% and 84 ± 13%. Amine nanoparticles, however, showed a pronounced and concentration-dependent cytotoxicity, with only 47 ± 1% cell viability at the highest concentration after 30 min. It should be noted that carboxy (100 nm) nanoparticles have been discontinued by the supplier prior to the onset of this study.

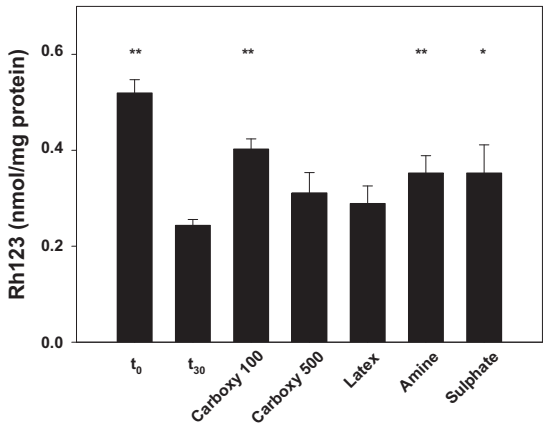

Fig. 4. Effect of different nanoparticles (100 μg/ml) on rhodamine 123 (Rh123) release from A549 cell layers cultured for 5 days. Cell layers were loaded with Rh123 (10 μM) for 30 min (t_0), and fluorescence was measured after another 30 min of release (t_{30}). Results are expressed as means ± SD from 6 independent experiments. $^*P < 0.05$, $^{**}P < 0.01$ versus control buffer alone.

3.4. Physicochemical characteristics of nanoparticles

Latex nanoparticles with various surface charges, surface modifications and sizes (see Table 1) were used in Rh123 release studies. Table 2 shows the changes in ζ-potential and particle size when analysing the NPs before and after release studies.

Prior to experiments, carboxy 100 and 500, latex and sulphate NPs were measured to be negatively charged with their ζ-potential values ranging from −22 to −63 mV. Amine-modified particles showed a net positive charge of 61 mV.

The particle sizes measured in our laboratory were in good agreement with the supplier's given specifications.

Incubation with A549 cell layers resulted in dramatic changes in both particle size and surface charge (Table 2). Whilst the ζ-potential was diminished among all nanoparticles, particle size increased significantly as a result of agglomeration. The highest increase was observed for amine-modified particles that grew from approximately 50 nm to almost 4 μm in diameter.

3.5. Western blot analysis

Nanoparticles suspended in KRB were incubated with A549 cell monolayers for 30 min, and the level of P-gp was quantified in the cells and the cell supernatant by Western blot (Fig. 6). No obvious changes in cellular P-gp levels, compared to control, were observed after incubation with the different nanoparticles (Fig. 6A). Extraction of P-gp from the membrane into the cell supernatant could also be ruled out, as no protein signals were obtained in the investigated samples (Fig. 6B).

3.6. Confocal laser scanning microscopy

The interactions of nanoparticles with A549 cell layers were observed using confocal laser scanning microscopy (Fig. 7). TRITC-labelled phalloidin was used to visualise the cytoskeleton. Agglomerated carboxy and sulphate NPs appeared in the same channel due to their Texas-red label (Fig. 7B and E). It is evident from the CLSM micrographs that none of the nanoparticles were taken up into the cells or caused significant disruption of the cytoskeleton.

Table 1
Physicochemical properties of nanoparticles used in the study.

Latex bead nanoparticles (Sigma–Aldrich order no.)	Abbreviation	Fluorescence label (excitation/emission)
Carboxylate-modified, 2.5% solids, 100 nm (L3405)	Carboxy 100	(575 nm/610 nm)
Carboxylate-modified, 2.5% solids, 500 nm (L3280)	Carboxy 500	(575 nm/610 nm)
Unmodified, 10% solids, 100 nm (LB1)	Latex	None
Amine-modified, 2.5% solids, 50 nm (L0780)	Amine	(360 nm/420 nm)
Sulphate-modified, 2.5% solids, 100 nm (L9902)	Sulphate	(575 nm/610 nm)

Table 2
Physicochemical properties of latex nanoparticles before and after rhodamine 123 release experiments.

Nanoparticles	Initial values			After Rh123 release		
	Size (nm)	PdI	ζ-potential (mV)	Size (nm)	PdI	ζ-potential (mV)
Carboxy 100	120.8 ± 0.4	0.02	−45.0 ± 0.5	563.4 ± 23.3	0.56	−20.6 ± 0.5
Carboxy 500	476.8 ± 9.2	0.07	−63.1 ± 0.4	2125.0 ± 117.9	0.32	−15.1 ± 0.8
Latex	117.1 ± 1.2	0.04	−48.5 ± 0.6	1715.0 ± 56.2	0.62	−42.2 ± 0.8
Amine	56.7 ± 0.8	0.05	61.3 ± 5.2	3943.0 ± 220.9	0.73	11.0 ± 0.8
Sulphate	131.1 ± 2.1	0.01	−22.3 ± 1.1	1422.0 ± 58.7	0.52	−10.0 ± 0.7

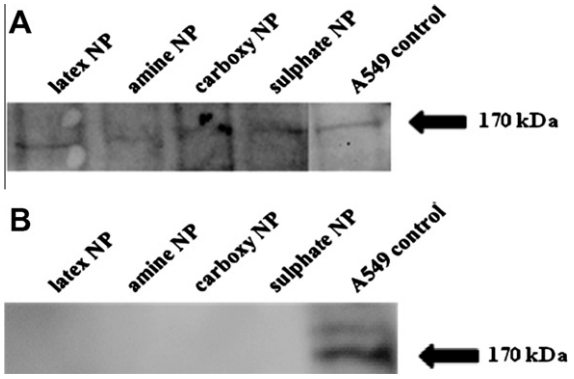

Fig. 6. Analysis of P-glycoprotein/MDR1 protein levels in A549 cells and supernatant. A549 cell layers were cultured for 5 days, before being incubated with different nanoparticles (100 μg/ml) for 30 min. Protein was extracted from cells and cell supernatant and probed with a monoclonal anti-P-gp antibody. (A) Representative immunoblot of cell lysate. A single band of 170 kDa can be detected in A549 cell lysate. (B) Representative immunoblot of cell supernatants. No signal could be obtained.

4. Discussion

Consistent with earlier observations [17,18], our data confirmed that the A549 cell line functionally expressed P-glycoprotein/MDR1. Rh123 efflux was found to be mediated by a saturable, single transporter site, and an increased accumulation of Rh123 was observed in the presence of verapamil, cyclosporine A and NaN_3/DOG, agents known to inhibit P-gp function and deplete ATP, respectively.

When studying the interaction of insoluble, latex-based nanoparticles of different surface modification, ζ-potential and particle size with P-gp, we found that Rh123 efflux from A549 cell layers was inhibited in a size- and surface-chemistry-dependant manner that, in some cases, was of similar scale as the attenuation observed with the pharmacological agents. These findings allow the speculation that nanoparticles might directly interfere with P-gp function. In particular, small, carboxylated and sulphated NPs were able to reduce P-gp-mediated efflux of Rh123 from A549 cells. Whilst similar effects were also observed for amine-modified particles, it cannot be ruled out that this effect resulted from the particles' acute cytotoxicity rather than from direct P-gp inhibition.

Recently, Arvizo et al. [19] reported that gold nanoparticles, depending on their surface charge, caused changes in membrane potential. Nevertheless, P-gp function has repeatedly been observed to be independent of membrane potential [20]. McCarthy and co-workers [21] have shown that when Calu-3 cell monolayers were acutely exposed to carbon nanoparticles, there was an inhibition of forskolin-induced I_{sc} activation through CFTR. They concluded that size and charge were essential factors in determining the extent of this effect and that cholesterol and specialised membrane domains at the cell surface play a pivotal role. Thus, a more direct interaction between the nanoparticles and the membrane or even the ABC transporter can be suggested to be responsible for the observed effects.

We observed that positively charged nanoparticles had the highest cytotoxicity, which is consistent with previous reports [19,22], whereas negatively charged nanoparticles induced only marginal cell death. Thus, whilst nanoparticles potentially change the conformation of the cell membrane, resulting in the disruption of cellular processes and membrane integrity [23,24], most interactions with the cell membrane do not cause any membrane disruption or extraction of the protein from the plasmalemma, as previously observed in the case of cyclodextrins [25]. This was confirmed by Western blot analysis of the cells and their supernatant.

Significant changes in the size of nanoparticles once they were in contact with the cell supernatant were shown. In most cases, the surface of nanoparticles is covered immediately after contact with biological fluids by several biomolecules [26]. The particles' surface interacts with its dispersion medium in a complex fashion, involving conflictive forces, especially between particles, ions and biological substances in the medium such as proteins. This interplay affects both the hydrodynamic size and the ζ-potential of the nanoparticles and can have an impact on the agglomeration statues of the particle itself [26].

To further our understanding of nanomedicines, it is necessary to investigate the nanomaterial's physicochemical properties and how these properties influence their uptake and biodistribution. This is the first study comparing pharmacological P-gp inhibitors with nanoparticulates. The attenuation of Rh123 release, and hence P-gp function by nanoparticles, is an interesting observation, which might further increase the interest in nanoparticulate drug delivery systems, particularly for the treatment of cancer and to overcome biological barriers imposed by efflux pumps, such as P-glycoprotein.

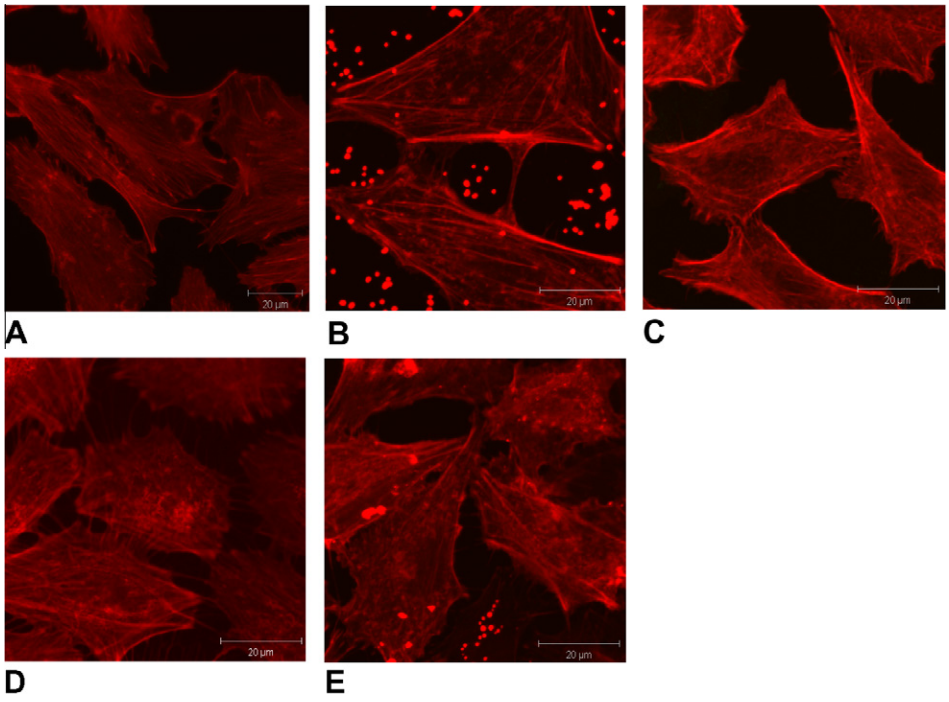

Fig. 7. Visualisation of F-actin in plastic-grown A549 human alveolar epithelial cell layers after 5 days of culture. Cells were plated at a density of 3.5×10^4 cells per cm^2 and cultured under liquid-covered culture conditions. Cells were fixed and labelled using TRITC-phalloidin (red), after being incubated with different nanoparticles (100 μg/ml) for 30 min. (A) Control, (B) carboxylated nanoparticles 500 nm, (C) unmodified latex nanoparticles, (D) amine-modified nanoparticles and (E) sulphate-modified nanoparticles. In (C) and (E), nanoparticles are visible due to their Texas-red label. Scale bars represent μm.

Acknowledgements

The authors acknowledge funding by a Strategic Research Cluster Grant (07/SRC/B1154) under the National Development Plan co-funded by EU Structural Funds and Science Foundation Ireland.

References

[1] S. Bhaskar, F. Tian, T. Stoeger, W. Kreyling, J.M. de la Fuente, V. Grazú, P. Borm, G. Estrada, V. Ntziachristos, D. Razansky, Multifunctional nanocarriers for diagnostics, drug delivery and targeted treatment across blood–brain barrier: perspectives on tracking and neuroimaging, Part, Fibre Toxicol. 7 (2010) 3.
[2] J. Sitterberg, A. Özcetin, C. Ehrhardt, U. Bakowsky, Using atomic force microscopy for the characterisation of nanoscale drug delivery systems, Eur. J. Pharm. Biopharm. 74 (2010) 2–13.
[3] K. Cho, X. Wang, S. Nie, Z.G. Chen, D.M. Shin, Therapeutic nanoparticles for drug delivery in cancer, Clin. Cancer Res. 14 (2008) 1310–1316.
[4] H. Bakowsky, T. Richter, C. Kneuer, D. Hoekstra, U. Rothe, C. Ehrhardt, U. Bakowsky, Adhesion characteristics and stability assessment of lectin-modified liposomes for site-specific drug delivery, Biochim. Biophys. Acta 1778 (2008) 242–249.
[5] E.S. Lee, K. Na, Y.H. Bae, Doxorubicin loaded pH-sensitive polymeric micelles for reversal of resistant MCF-7 tumor, J. Control. Release 103 (2005) 405–418.
[6] T. Thomas, T. Bahadori, N. Savage, K. Thomas, Moving toward exposure and risk evaluation of nanomaterials: challenges and future directions, Wiley Interdiscip. Rev. Nanomed. Nanobiotechnol. 1 (2009) 426–433.
[7] B.C. Baguley, Multidrug resistance in cancer, Methods Mol. Biol. 596 (2010) 1–14.
[8] B. Bauer, A.M. Hartz, G. Fricker, D.S. Miller, Modulation of p-glycoprotein transport function at the blood–brain barrier, Exp. Biol. Med. (Maywood 23) (2005) 118–127.
[9] L.Z. Benet, The drug transporter-metabolism alliance: uncovering and defining the interplay, Mol. Pharm. 6 (2009) 1631–1643.
[10] F. Frezard, E. Pereira-Maia, P. Quidu, W. Priebe, A. Garnier-Suillerot, P-glycoprotein preferentially effluxes anthracyclines containing free basic versus charged amine, Eur. J. Biochem. 268 (2001) 1561–1567.
[11] C. Bosquillon, Drug transporters in the lung-implication in the biopharmaceutics of inhaled drugs, J. Pharm. Sci. 99 (2009) 2240–2255.
[12] S. Endter, U. Becker, N. Daum, H. Huwer, C.M. Lehr, M. Gumbleton, C. Ehrhardt, P-glycoprotein (MDR1) functional activity in human alveolar epithelial cell monolayers, Cell. Tissue Res. 328 (2007) 77–84.
[13] D. Francombe, G. Taylor, S. Taylor, G. Somers, C.D. Edwards, M. Gumbleton, Functional role of P-gp efflux in limiting pulmonary drug absorption within an intact lung: application of an isolated perfused rat lung model, Respir. Drug Deliv. 11 (2008) 461–464.
[14] F. Manford, Y. Riffo-Vasquez, D. Spina, C. P Page, A.J. Hutt, V. Moore, F. Johansson, B. Forbes, Lack of difference in pulmonary absorption of digoxin, a P-glycoprotein substrate, in mdr1a-deficient and mdr1a-competent mice, J. Pharm. Pharmacol. 60 (2008) 1305–1310.
[15] D.J. Giard, S.A. Aaronson, G.J. Todaro, P. Arnstein, J.H. Kersey, H. Dosik, W.P. Parks, *In vitro* cultivation of human tumors: establishment of cell lines derived from a series of solid tumors, J. Natl. Cancer Inst. 51 (1973) 1417–1423.
[16] J.L. Sporty, L. Horálková, C. Ehrhardt, *In vitro* cell culture models for the assessment of pulmonary drug disposition, Expert Opin. Drug Metab. Toxicol. 4 (2008) 333–345.
[17] K. Hamilton, G. Backstrom, M.A. Yazdanian, K.L. Audus, P-glycoprotein efflux pump expression and activity in Calu-3 cells, J. Pharm. Sci. 90 (2000) 647–658.
[18] T. Lehmann, C. Köhler, E. Weidauer, C. Taege, H. Foth, Expression of MRP1 and related transporters in human lung cells in culture, Toxicology 167 (2001) 59–72.
[19] R.R. Arvizo, O.R. Miranda, M.A. Thompson, C.M. Pabelick, R. Bhattacharya, J.D. Robertson, V.M. Rotello, Y.S. Prakash, P. Mukherjee, Effect of nanoparticle surface charge at the plasma membrane and beyond, Nano Lett. 10 (2010) 2543–2548.
[20] G.D. Luker, T.P. Flagg, Q. Sha, K.E. Luker, C.M. Pica, C.G. Nichols, D. Piwnica-Worms, MDR1 P-glycoprotein reduces influx of substrates without affecting membrane potential, J. Biol. Chem. 276 (2001) 49053–49060.
[21] J. McCarthy, M. Duszyk, M. Radomski, Effect of nanoparticulate matter on transepithelial ion fluxes in Calu-3 cells, Am. J. Respir. Crit. Care Med. 179 (2009) A5041.
[22] M. Lundqvist, J. Stigler, G. Elia, I. Lynch, T. Cedervall, K.A. Dawson, Nanoparticle size and surface properties determine the protein corona with possible implications for biological impacts, Proc. Natl. Acad. Sci. USA 105 (2008) 14265–14270.
[23] I. Lynch, T. Cedervall, M. Lundqvist, C. Cabaleiro-Lago, S. Linse, K.A. Dawson, The nanoparticle-protein complex as a biological entity; a complex fluids and surface science challenge for the 21st century, Adv. Colloid Interface Sci. 31 (2007) 167–174.
[24] R. Foldbjerg, D.A. Dang, H. Autrup, Cytotoxicity and genotoxicity of silver nanoparticles in the human lung cancer cell line, A549, Arch. Toxicol. (2010), doi:10.1007/s00204-010-0545-5 (Epub ahead of print).
[25] S.W. Kamau, S.D. Krämer, M. Günthert, H. Wunderli-Allenspach, Effect of the modulation of the membrane lipid composition on the localization and function of P-glycoprotein in MDR1-MDCK cells, In Vitro Cell Dev. Biol. Anim. 41 (2005) 207–216.
[26] I. Lynch, A. Salvati, K.A. Dawson, Protein-nanoparticle interactions: what does the cell see?, Nat Nanotechnol. 4 (2009) 546–547.